5 Hepatobiliary, Pancreas, Adrenal, Melanoma, and GIST

Heidi Wassef and Linh T. Ho

Case 5.1

History

A 55-year-old man with recently diagnosed hepatocellular carcinoma (HCC). PET-CT requested for staging.

Findings

The small HCC is associated with focal enhancement at the dome of the liver on the contrast-enhanced axial image (Fig. 5.1a) but is not appreciated on the non-contrast-enhanced image (Fig. 5.1b). The HCC is not associated with hypermetabolism as shown on the fused PET-CT image (Fig. 5.1c) and the FDG PET image (Fig. 5.1d). Contrast-enhanced CT would be the follow-up study of choice since this HCC is not ^{18}F-FDG avid.

Pearls and Pitfalls

- The reported sensitivity of PET-CT for the detection of HCC is 55 % while for CT is 90 %, thus CT with IV contrast is the preferred study for diagnosis, staging, and restaging of HCC.
- Hypermetabolism in the hepatic tissue adjacent to a lesion can be seen up to 3 months following transarterial chemoembolization as a reaction to the infarcted tumor.
- Mild hypermetabolism in the parenchyma peripheral to the tumor occurs 2–3 days following radiofrequency ablation (RFA). The recommended ideal imaging time is 24–48 h following RFA because the cellular damage caused by thermocoagulation in RFA is immediate.

P.S. Conti, A. Kaushik (eds.), *PET-CT*, DOI 10.1007/978-1-4419-5811-2_5

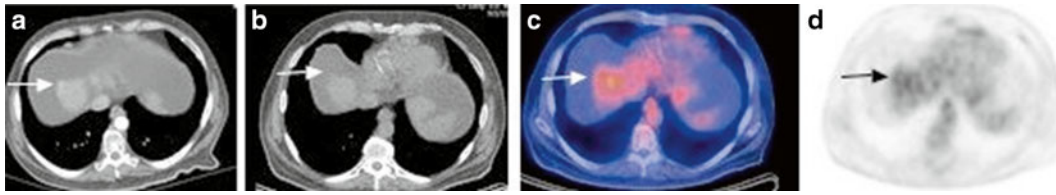

Fig. 5.1

Discussion

PET-CT has low sensitivity for the detection of HCC partly due to the high levels of glucose-6-phosphatase in the liver which dephosphorylates FDG-6-PO4 allowing it to leave the cell. Unlike the liver, other tissue do not have glucose-6-phosphatase, and thus FDG-6-PO4 is trapped within the cell allowing radiotracer accumulation and visualization. High-grade HCCs are less well differentiated and thus have less glucose-6-phosphatase.

Every year, there are nearly half a million people diagnosed with HCC. HBV or HCV infections and probably nonalcoholic liver disease are risk factors for HCC. The most common sites of extrahepatic metastatic HCC are the lung, abdominal lymph nodes, and bone.

Case 5.2

History

A 75-year-old man with newly diagnosed gallbladder carcinoma. PET-CT was requested to evaluate for metastatic disease.

Findings

A 2.7×1.4 cm intensely active soft tissue lesion within the gallbladder (Fig. 5.2), with SUVmax of 5.7, represents the primary neoplasm. In addition, there is mild wall thickening of the gallbladder with pericholecystic fluid, with no definite discernible activity, probably due to inflammation.

Several celiac axis (Fig. 5.2), retroperitoneal, and retrocrural lymph nodes are seen, consistent with metastases. The largest celiac axis adenopathy (near the stomach) measures 1.6×1.7 cm and has a SUVmax of 5.6.

Pearls and Pitfalls

- PET-CT is valuable for detecting regional lymph node involvement and distant metastases that are not diagnosed by multi-detector CT (MDCT).
- PET-CT shows no significant advantage over MDCT for the diagnosis of the primary gallbladder tumor.
- PET is helpful in detecting residual gallbladder carcinoma after cholecystectomy but has low sensitivity for detecting carcinomatosis.

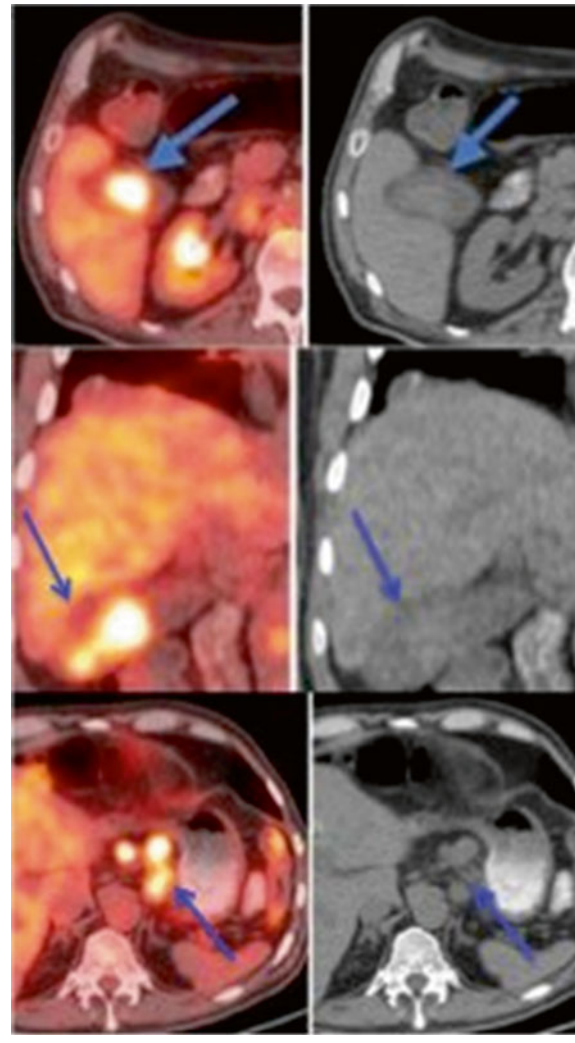

Fig. 5.2

Discussion

PET-CT shows a significantly higher positive predictive value (94.1 % vs. 77.5 %, $p = 0.04$) than that found for MDCT in the diagnosis of regional lymph node metastasis. In addition, PET-CT also demonstrates a significantly higher sensitivity (94.7 % vs. 63.2 %, $p = 0.02$) than MDCT in the diagnosis of distant metastases. A SUVmax of 3.65 was found to be the best cutoff value for detecting a gallbladder malignant tumor. PET-CT findings resulted in a change of management in 17 % of patients deemed resectable after standard workup.

Case 5.3

History

A 67-year-old man underwent an ERCP with biopsy revealing cholangiocarcinoma. PET-CT requested for staging.

Findings

There is an ill-defined, intensely hypermetabolic large mass involving the medial segment of the left lobe and the anterior segment of the right lobe of the liver (Fig. 5.3, arrowheads), consistent with the known cholangiocarcinoma (CC). The tumor likely involves and engulfs the gallbladder due to the apparent indistinctness of the gallbladder wall. A small, active hepatoduodenal lymph node is present (not shown). In addition, there is also mild hypermetabolism involving the entire pancreas (Fig. 5.3, arrows) due to post-ERCP pancreatitis. Hypermetabolism surrounding the biliary stent is due to foreign body reaction, but in this case, there may also be tumor involvement.

Pearls and Pitfalls

- PET-CT is valuable for detecting regional lymph node involvement and unsuspected distant metastases that are not diagnosed by MDCT.
- Hypermetabolism could be seen in patients with primary sclerosing cholangitis or known granulomatous disease as well as biliary stents, which could mimic neoplasm.

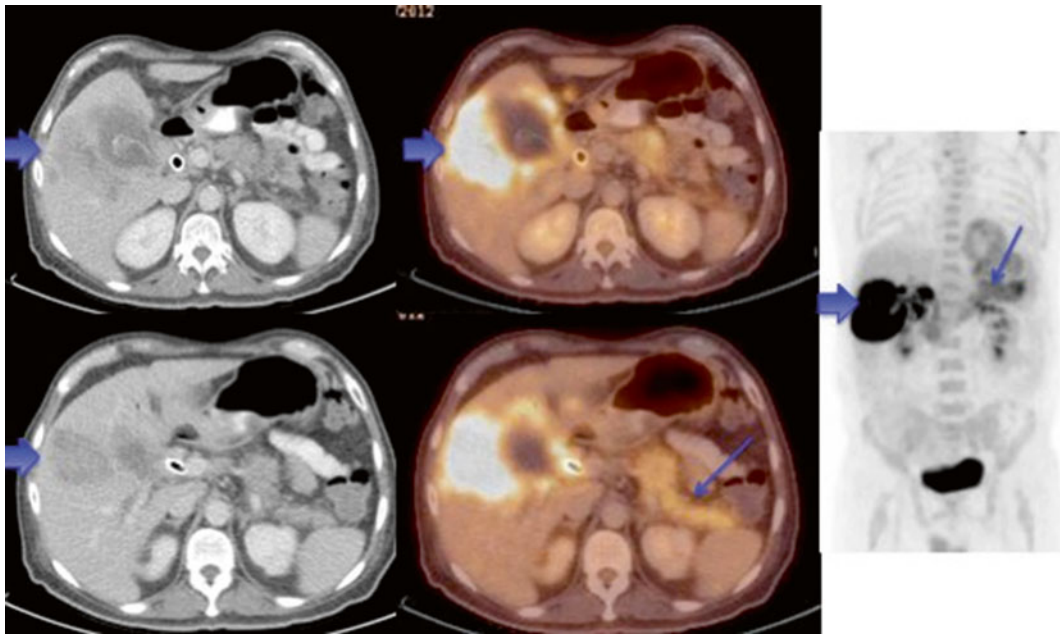

Fig. 5.3

Discussion

For cholangiocarcinoma, PET-CT shows significantly higher accuracy over CT in the diagnosis of regional lymph nodes (75.9 % vs. 60.9 %, $p = 0.004$) and distant metastases (88.3 % vs. 78.7 %, $p = 0.004$). There is no significant advantage of PET-CT over multi-detector CT (MDCT) for the diagnosis of a primary biliary tumor. FDG PET was shown to change management in 30 % of patients with CC. Additionally, FDG PET-CT is useful in patients with CC (except for infiltrating type) for detection of recurrent disease and for assessment of treatment response.

Case 5.4

History

A 73-year-old woman with recently discovered pancreatic head mass.

Findings

There is a $7 \times 7 \times 4$ cm hypermetabolic pancreatic head mass with a SUVmax of 13 (Fig. 5.4).

Pearls and Pitfalls

- For accurate staging of pancreatic carcinoma, the size of the tumor, relationship to adjacent vessels, and invasion of nearby tissue and spread of disease outside the pancreas must be assessed. Endoscopic ultrasound (EUS) has been found to be more accurate than CT in local staging of pancreatic malignancies and in predicting vascular invasion and resectability.
- Pancreatic cancer spreads to regional lymph nodes followed by the liver and lung. Osseous metastases are rare.
- PET can reliably detect hepatic, peritoneal, and other distant metastases that are at least 1 cm.

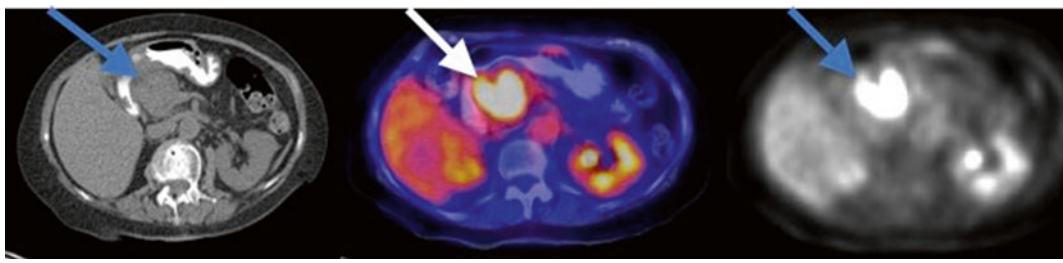

Fig. 5.4

Discussion

The pancreatic head is defined as the segment to the right of the left border of the superior mesenteric vein (SMV). The body extends from the left border of the SMV to the left border of the aorta. The narrow segment between the head and body is defined as the neck. The segment of pancreas posterior to the SMV is the uncinate process. PET-CT is helpful in differentiating benign and malignant pancreatic masses using a SUVmax cutoff of 2.5.

Case 5.5

History

Patient had a Whipple procedure for moderately differentiated pancreatic adenocarcinoma. PET-CT performed to assess response following chemotherapy.

Findings

There is peripheral increased FDG uptake at the liver surface (Fig. 5.5) with SUVmax up to 5.3 consistent with peritoneal carcinomatosis. Some of the foci of hypermetabolism demonstrate no CT correlate and some show peritoneal thickening or nodularity.

Pearls and Pitfalls

Peritoneal metastases can appear to lie within the liver. Careful evaluation of the coronal and sagittal images is helpful in differentiating peritoneal implants from peripheral hepatic lesions particularly if the peritoneal deposits are not evident on CT.

Discussion

Tumors that may involve the peritoneal cavity include malignant peritoneal mesothelioma, pseudomyxoma peritonei, and metastases from the stomach, colon, appendix, gallbladder, pancreas, ovary, breast, lung, uterus, and lymphoma. CT has a sensitivity of 43 % and positive predictive value of 100 % for evaluation of peritoneal carcinomatosis, while PET-CT has a sensitivity of 78 % and positive predictive value of 96 %.

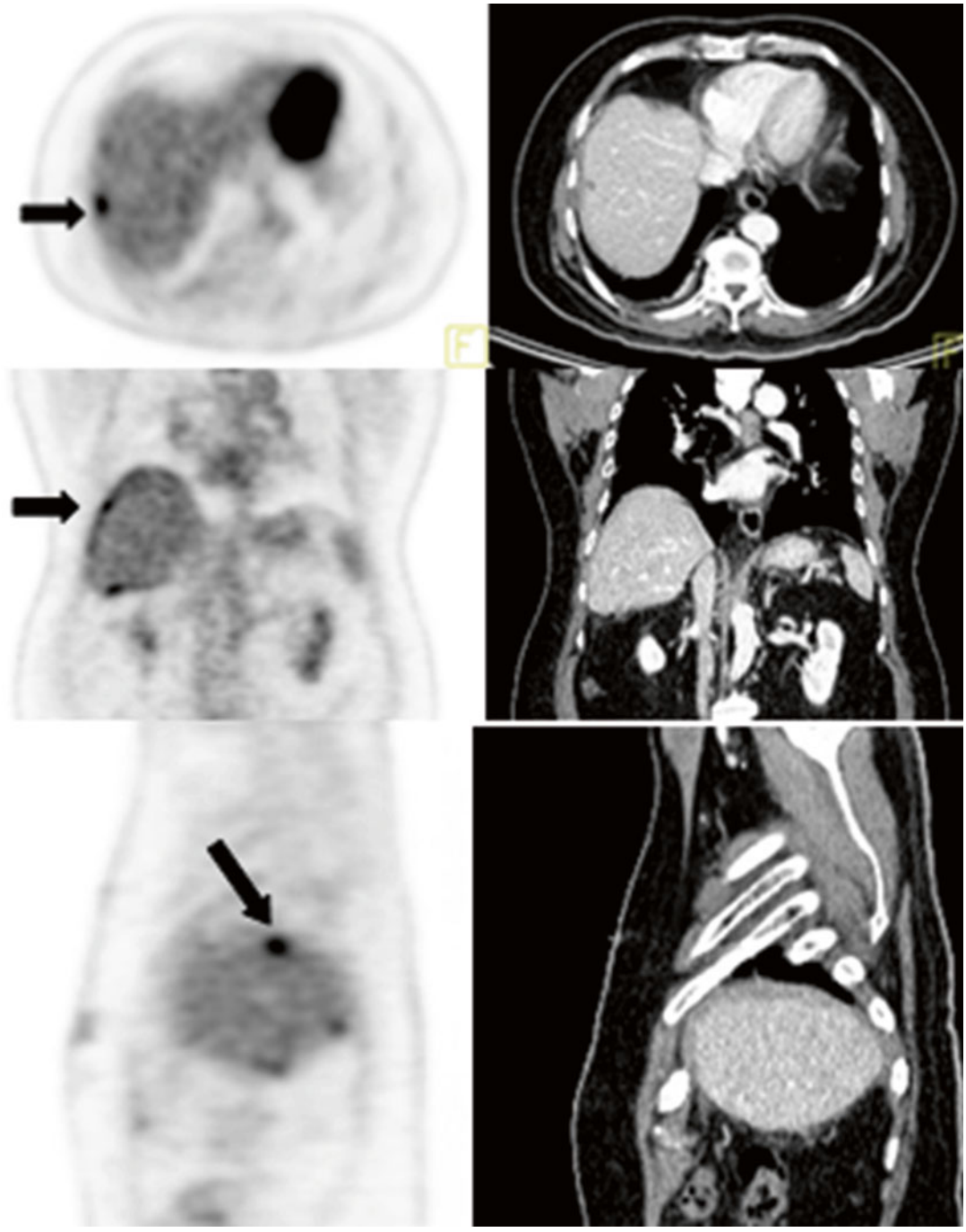

Fig. 5.5

Case 5.6

History

Patient with moderately differentiated adenocarcinoma of the ampulla who is status post hepaticojejunostomy, right hemicolectomy, and partial hepatectomy in February 2010 had his last chemotherapy dose 2 months ago.

Findings

Patient had interval progression of right paratracheal and precarinal adenopathy and interval development of multiple right axillary and subpectoral nodes.

Pearls and Pitfalls

The histological differentiation of periampullary cancer is more important than the anatomical location. Pancreatobiliary histology carries a worse prognosis than intestinal histology in periampullary cancers.

Discussion

Periampullary cancers can arise from the pancreas, duodenum, distal common bile duct (CBD), or the ampullary duct. Ampullary carcinoma most commonly presents as obstructive jaundice in 80 % of patients and is treated with a Whipple procedure (pancreaticoduodenectomy). Pneumonia, abdominal infection, anastomotic leaks, and delayed gastric emptying are the most common complications following a Whipple procedure.

Case 5.7

History

Woman diagnosed with pancreatic cancer. PET-CT requested for staging.

Findings

A solitary focus of hypermetabolism was consistent with hepatic metastases (Fig. 5.6).

Pearls and Pitfalls

Hepatic metastasis appeared as a vertically oriented linear lesion due to patient breathing.

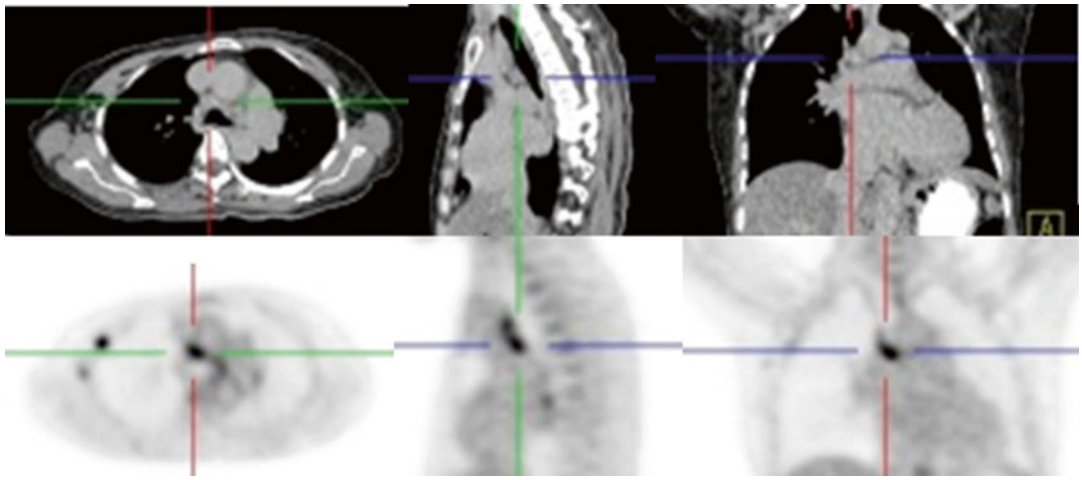

Fig. 5.6

Discussion

Only 15–20 % of patients with pancreatic cancer are resectable at diagnosis and have a 20 % 5-year survival rate. Gallium-68 DOTATATE positron emission tomography/computed tomography (PET-CT neuroendocrine tumors) changed therapy in 35 % of patients Pancreatic ductal adenocarcinomas are characterized by invasiveness, rapid progression and resistance to treatment. Potentially curative resection followed by adjuvant systemic chemotherapy is the most common therapeutic strategy.Pancreatic cancer has a proclivity for perineural invasion. It is characterized by lymphatic spread to adjacent and distant lymph nodes and metastases to the liver, peritoneum and the lung. Higher metabolic activity on FDG PET correlates with higher initial stage of pancreatic adenocarcinoma and with decreased overall survival.

Case 5.8

History

A 61-year-old male with history of gastrointestinal stromal tumor (GIST) for follow-up evaluation.

Findings

The patient is status post partial gastrectomy and splenectomy. There is interval development of a hypermetabolic focus in the caudate lobe (segment 1) consistent with recurrent disease (Fig. 5.7).

Pearls and Pitfalls

PET-CT can predict malignant potential of GISTs. An SUV greater than 5 indicates a higher likelihood of having a malignant potential.

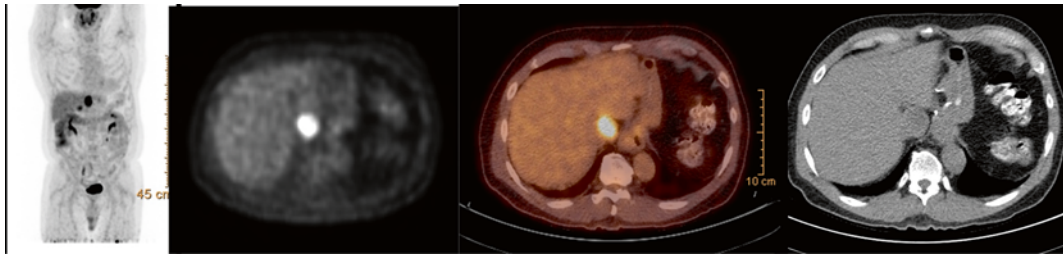

Fig. 5.7

Discussion

PET-CT no earlier than 6–8 weeks following GIST resection improves the diagnostic accuracy and influences treatment. Studies performed less than 6 weeks following resection have a higher incidence of false-negative, false-positive, and indeterminate findings.

Case 5.9

History

A 64-year-old male diagnosed with GIST 7 years ago. The patient is on sixth line chemotherapy. PET-CT requested to evaluate response to chemotherapy.

Findings

Hypermetabolic metastases are seen in the posterior segment of the right lobe and lateral segment of the left lobe (Fig. 5.8, arrows). Although the lesions as seen on CT are unchanged in size compared to the prior study, the hypermetabolism has increased in size and activity. Patient was admitted due to bleeding. Hemoglobin became stable, and thus no surgical or radiologic interventional procedure was required.

Pearls and Pitfalls

The size of the lesion on a post-therapy scan as determined by CT is not an accurate assessment of response to therapy.

Discussion

A decrease in metabolic activity indicating response to therapy is seen weeks to months prior to a significant decrease in the size of the lesion. Post-chemotherapy studies revealing no change in metabolism indicates primary resistance of the tumor to the administered chemotherapy.

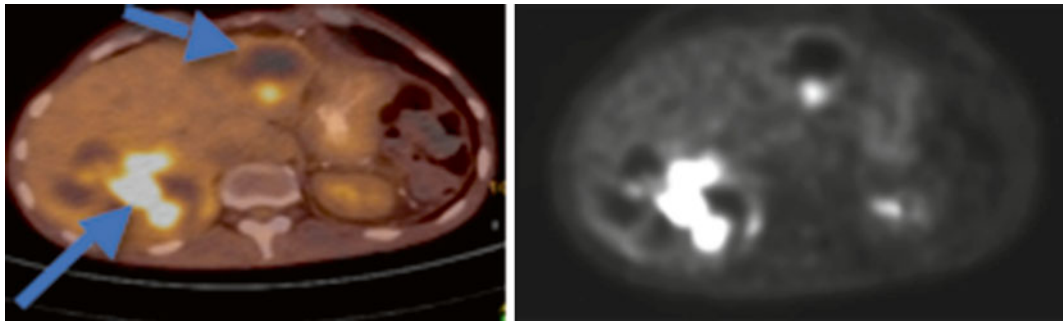

Fig. 5.8

Case 5.10

History

A 64-year-old man with esophageal adenocarcinoma. PET-CT is requested for staging.

Findings

There is diffuse esophageal wall thickening with intensely increased metabolic activity involving the distal 2/3 of the esophagus consistent with the reported recent diagnosis of esophageal adenocarcinoma via endoscopy. Multiple scattered hypermetabolic foci involving the liver, bone, retroperitoneal and cervical nodes, and right adrenal gland (Fig. 5.9, arrows) are consistent with metastases. There is also mild activity in the left adrenal gland which is physiologic.

Pearls and Pitfalls

Several groups have evaluated using a cutoff of 1 for the ratio of SUVmax of adrenal gland to SUVmax of the liver to differentiate benign from malignant adrenal lesions. Blake et al. found the sensitivity, specificity, positive predictive value, negative predictive value, and accuracy to be 100 %, 93.8 %, 81.8 %, 100 %, and 95.1 %, respectively. Potential false negatives include a very small malignant tumor, tumors with significant necrosis, and metastases from tumors with limited 18F-FDG uptake such as mucinous or neuroendocrine tumors. Potential false positives include rare hypermetabolic adenomas and pheochromocytoma. Ten percent of pheochromocytomas are malignant, 10 % are bilateral, 10 % are in children, and 10 % are extra-adrenal.

Discussion

An adrenal lesion with Hounsfield unit (HU) < 10 indicates a lipid-rich adenoma. If HU ≥ 10, 18F-FDG PET, CT washout test, magnetic resonance chemical shift imaging with in-phase and out-of-phase images, or

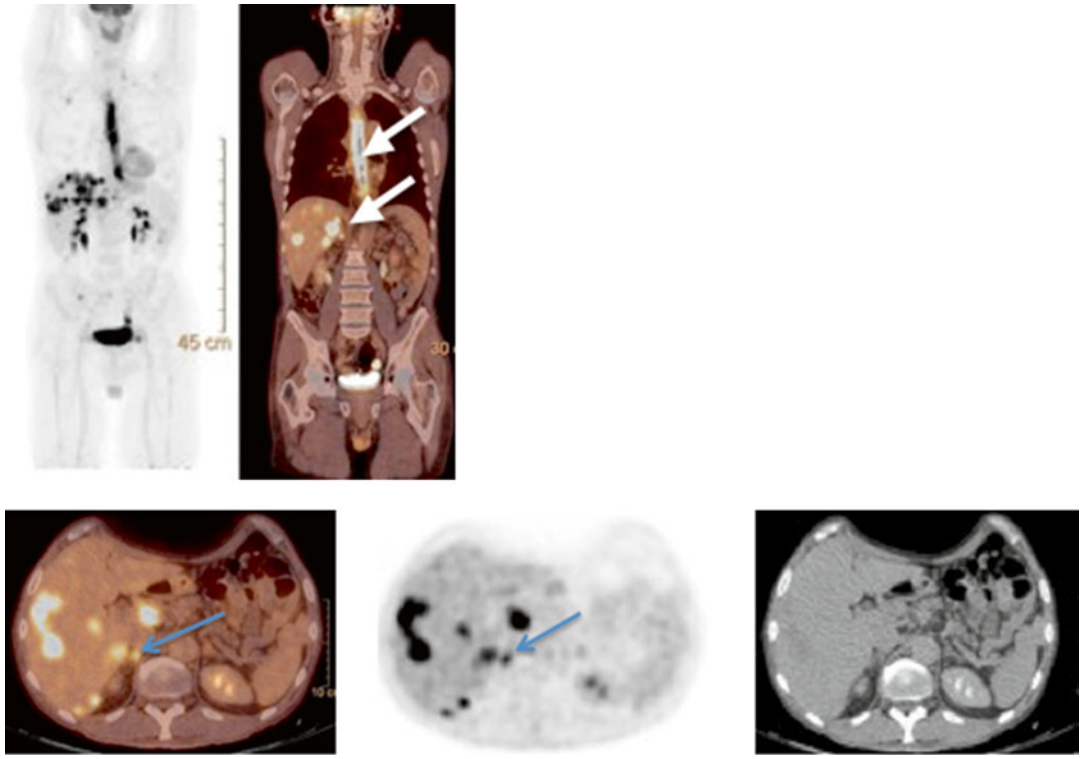

Fig. 5.9

biopsy may be used to differentiate between benign and malignant lesions. Greater than 60 % intravenous contrast washout at 15 min compared to uptake at 60 s in the adrenal lesion indicates that it is an adenoma.

Case 5.11

History

Newly diagnosed right adrenal cortical carcinoma.

Findings

There is an 8 cm heterogeneous, hypermetabolic mass superior to the right kidney (Fig. 5.10, arrows). There were no enlarged lymph nodes. Pathology examination revealed adrenal cortical carcinoma with lymphovascular invasion. Periaortic lymph nodes were negative.

Pearls and Pitfalls

Adrenal cortical carcinoma (ACC) is often large at presentation. ACC appears heterogeneous due to the presence of necrosis, hemorrhage, and

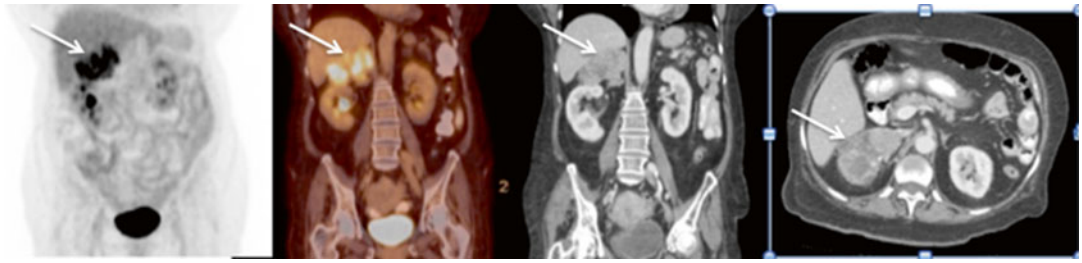

Fig. 5.10

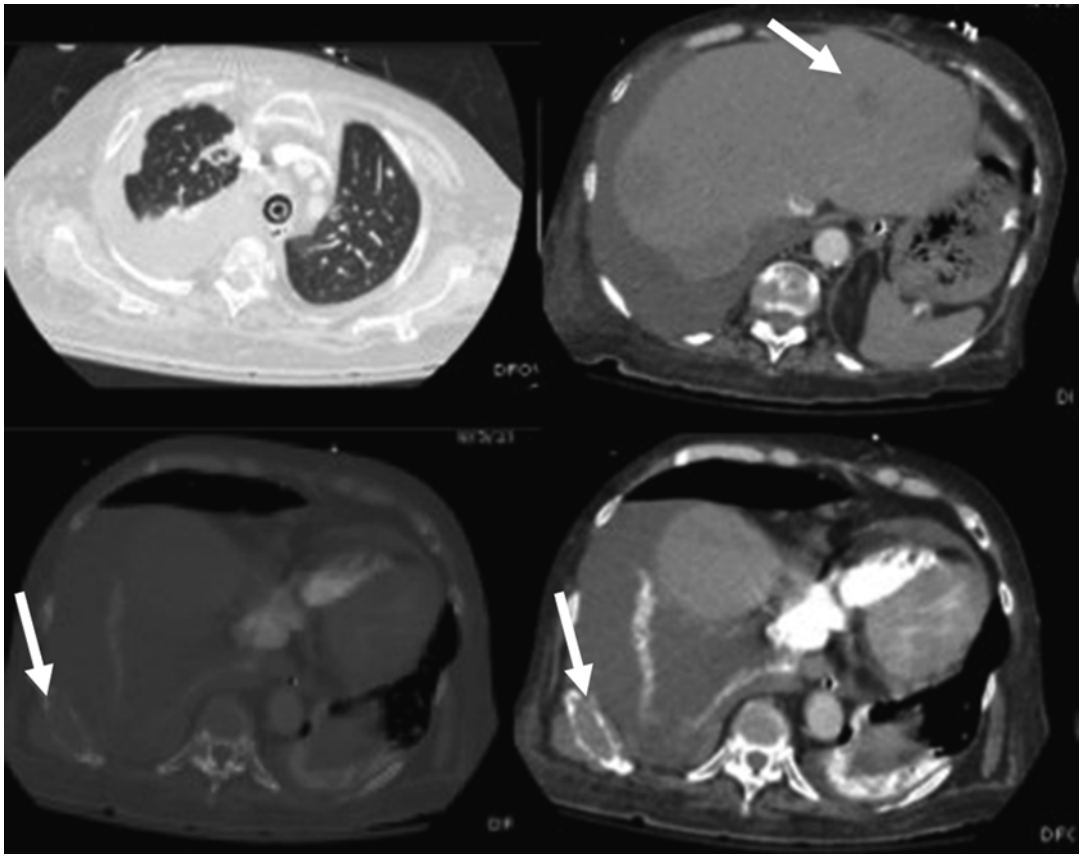

Fig. 5.11

calcification. Large tumors may invade the adrenal vein and inferior vena cava. Metastases commonly involve the lung, liver, and bone (Fig. 5.11, 1 year later) but can involve cervical and mediastinal lymph nodes, ovaries, pancreas, thyroid, brain, spleen, and peritoneum.

Discussion

ACC is rare with an incidence of 2 per million. Age of presentation is between 30 and 70 years. ACC may present due to excess hormone production or due to mass effect. Cushing's syndrome which involves excess

cortisol production may present with weak muscles, fat on the back of neck and upper back, abnormal hair growth, mood changes, high blood pressure, and high blood sugars. In most patients with ACC, detection of the first metastasis occurs within 4 months of diagnosis. Five-year survival drops to 0–24 % in patients with metastases compared to 58–66 % in patients without metastatic disease.

Case 5.12

History

A 51-year-old woman with recently diagnosed melanoma following shave biopsy overlying the left mandible. The patient has a palpable left cervical lymph node. PET-CT was requested for staging.

Findings

A 1 cm left cervical level 2 lymph node has a SUVmax of 2.2 (Fig. 5.12, arrows). This lymph node was biopsied revealing metastatic disease.

Pearls and Pitfalls

PET-CT has a high sensitivity and specificity in detecting distant metastases from melanoma. The sensitivity of PET-CT for the detection of melanoma in regional lymph nodes is reported to be only 16.7 %, and thus PET-CT cannot replace lymphoscintigraphy for evaluation of regional nodes. Reports indicate that PET-CT may aid in the detection of primary disease in patients with metastatic melanoma of unknown primary.

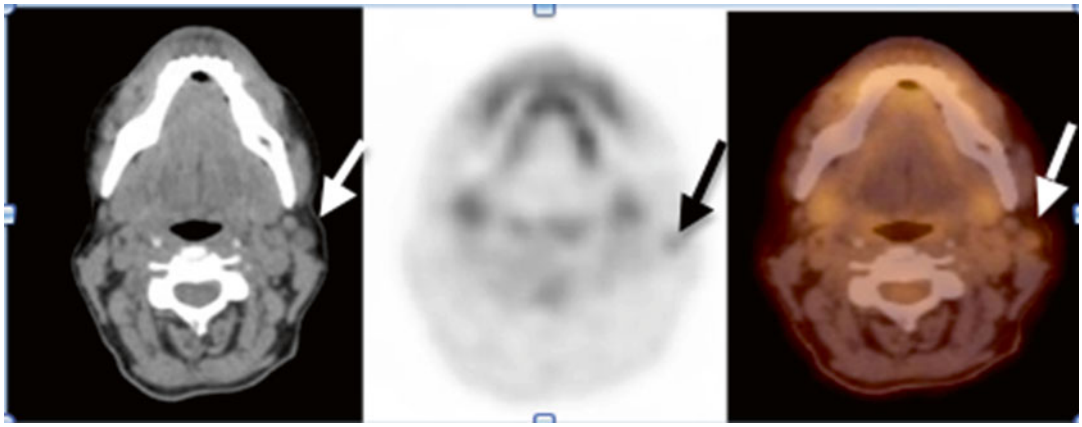

Fig. 5.12

Discussion

The T stage depends on the tumor thickness with lesions less than 1.0 mm thick, 1.01–2.0, 2.01–4.0, and >4.0 mm classified as T1, T2, T3, and T4, respectively. Sentinel lymph node (SLN) biopsy is recommended for patients with Breslow thickness 1–4 mm melanomas. Completion lymph node dissection is performed if the SLN is positive.

Case 5.13

History

A 64-year-old man who had resection 2 yrs ago of a 6 mm lentigo maligna subtype of melanoma on his left cheek with perineural and subcutaneous invasion. The patient underwent radiation 1 year ago. Restaging PET-CT is requested following chemotherapy to determine response to therapy.

Findings

There has been interval progression of disease with interval increase in size of hypermetabolic left cervical level 1B lymph node (Fig. 5.13, arrow) as well as increase in number of pulmonary nodules.

Pearls and Pitfalls

PET-CT has higher accuracy (97.2 %) than PEt alone (92.8 %) and CT alone (78.8 %) for N (lymph node) and M (metastases) staging. The sensitivity of PET-CT for the detection of pulmonary melanoma metastases depends on size. The sensitivity is 100 % for nodules 12 mm or larger, 63.6 % for 10–11 mm, 56.8 % for 8–9 mm, 33.3 % for 6–7 mm, and 7.9 % for 4–5 mm nodules.

Discussion

The most common location for melanoma is the upper back in men and the lower legs and upper back in women. Superficial spreading, lentigo maligna, nodular, and acral lentiginous are subtypes of melanoma that

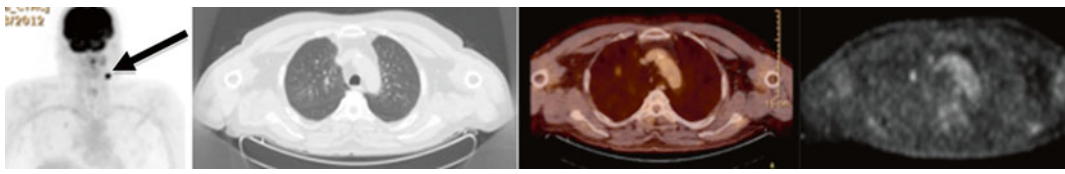

Fig. 5.13

are distinguished by their growth patterns. Review of the patient records is important. Recurrent disease in patients with stage I and II melanomas is most likely locoregional, while in stage III disease is likely distant. Common sites of metastases are the skin, subcutaneous tissue, lymph node, liver, bone, lung, brain, and visceral organs.

Suggested Reading

Anderson CD, Rice MH, Pinson CW, et al. Fluorodeoxyglucose PET imaging in the evaluation of gallbladder carcinoma and cholangiocarcinoma. J Gastrointest Surg. 2004;8(1):90–7.

Assie G, Antoni G, Tissier F, et al. Prognostic parameters of metastatic adrenocortical carcinoma. J Clin Endocrinol Metab. 2007;92(1):148–54.

Bertz-Lepel J, Rahm J, Pink D, et al. Influence of PET/CT on therapeutic management after resection of high-risk or very high-risk GIST. J. Clin Oncol 2011;29(suppl; abstr e20516).

Blake MA, Slattery JM, Kaira MK. Adrenal lesions: characterization with fused PET/CT image in patients with proved or suspected malignancy—initial experience. Radiology. 2006;238:970–7.

Chin BB, Wahl RL. 18F-Fluoro-2-deoxyglucose positron emission tomography in the evaluation of gastrointestinal malignancies. Gut. 2003;52 Suppl 4:iv23–9.

Chuang TY, Coleman 3rd JJ. Current therapy of cutaneous melanoma. Plast Reconstr Surg. 2001;105:1774–99.

Donghiui L, Keping X, Wolff R, et al. Pancreatic cancer. Lancet. 2004;363:15841–8.

Elsayes KM, Caoili EM. Adrenal imaging: a practical guide to diagnostic workup and spectrum of imaging findings. Appl Radiol. 2011;40(9):14–9.

El-Serag HB. Hepatocellular carcinoma. N Engl J Med. 2011;365(12):1118–27.

Ghazali N, Collyer JC, Tighe J. Navigation-assisted localisation and resection of subclinical metastatic malignant melanoma of unknown primary based on 18-fluorodeoxyglcose positron emission tomography computed tomography fusion imaging. Int J Oral Maxillofac Surg. 2012;14(1):5–8. Epub 2011 Oct 22.

Gress F, Hawes R, Thomas S, et al. Role of EUS in the preoperative staging of pancreatic cancer: a large single-center experience. Gastrointest Endosc. 1999;50:786–91.

Heinrick S, Pierre-Alain C. Ampullary cancer. Curr Opin Gastroenterol. 2010;26:280–5.

Icard P, Goudet P, Charpenay C, et al. Adrenocortical carcinomas: surgical trends and results of a 253-patient series from the French Association of Endocrine Surgeons study group. World J Surg. 2001;25:891–7.

Jadvar H, Henderson RW, Conti PS. [F-18]fluorodeoxyglucose positron emission tomography and positron emission tomography: computed tomography in recurrent and metastatic cholangiocarcinoma. J Comput Assist Tomogr. 2007;31(2):223–8.

Kim JY, Kim MH, Lee TY, et al. Clinical Role of ^{18}F-FDG PET-CT in suspected and potentially operable cholangiocarcinoma: a prospective study compared with conventional imaging. Am J Gastroenterol. 2008;103(5):1145–51.

Lee SW, Kim HJ, Park JH, et al. Clinical usefulness of 18F-FDG PET-CT for patients with gallbladder cancer and cholangiocarcinoma. J Gastroenterol. 2010;45(5):560–6.

Levy A, et al. Secondary tumors and tumorlike lesions of the peritoneal cavity: imaging features with pathologic correlation. Radiographics. 2009;29:347–73.

Mayerhoefer ME, Prosch H, Herold CJ, et al. Assessment of pulmonary melanoma metastases with (18)F-FDG PET/CT: which PET-negative patients require additional tests for definitive staging? Eur Radiol. 2012;22(11):2451–7.

Metser U, Miller E, Lerman H, et al. 18F-FDG PET/CT in the evaluation of adrenal masses. J Nucl Med. 2006;47(1):32–7.

Petrowsky H, Wildbrett P, Husarik DB, et al. Impact of integrated positron emission tomography and computed tomography on staging and management of gallbladder cancer and cholangiocarcinoma. J Hepatol. 2006;45(1):43–50.

Purandare NC, Rangarajan V, Shah SA, et al. Therapeutic response to radiofrequency ablation of neoplastic lesions: FDG PET/CT findings. Radiographics. 2011;31(1): 201–13.

Romano E, Scordo M, Dusza SW, et al. Site and timing of first relapse in stage III melanoma patients: implications for follow-up guidelines. J Clin Oncol. 2010;28(18): 3042–7. Epub 2010 May 17.

Ryan D, Mamon H, Fernandez-del Castillo C. Ampullary carcinoma: treatment and prognosis. http://www.uptodate.com/contents/ampullary-carcinoma-treatment-and-prognosis. Accessed 19 Nov 2012.

Tamm EP, Fleming JB, Varadhachary GR. In: Silverman P, editor. Oncologic imaging: a multidisciplinary approach. Elsevier, Philadelphia; 2012.

Turlakow A, et al. Peritoneal carcinomatosis: role of 18F-FDG PET. J Nucl Med. 2003;44:1407–12.

Van den Abbeele AD. The lessons of GIST-PET and PET/CT: a new paradigm for imaging. Oncologist. 2008;13 Suppl 2:8–13.

Wagner JD, Schauwecker D, Davidson D, et al. Prospective study of fluorodeoxyglucose-positron emission tomography imaging of lymph node basins in melanoma patients undergoing sentinel node biopsy. J Clin Oncol. 1999;17(5):1508–15.

Wagner JD, Gordon MS, Jaeger U, et al. Diagnostic performance of whole body dual modality 18F-FDG PET/CT imaging for N- and M-staging of malignant melanoma: experience with 250 consecutive patients. J Clin Oncol. 2006;24(7):1178.

Wong SL, Balch CM, Agarwala SS, et al. Sentinel lymph node biopsy for melanoma: American Society of Clinical Oncology and Society of Surgical Oncology Joint Clinical Practice Guideline. Ann Surg Oncol. 2012;19(11):3313–24.

Yoshikawa K, Shimada M, Sato H, et al. The utility of PET-CT in predicting malignant potential of GIST. J Clin Oncol 2012;30(suppl 4, abstr 38)